PREDICTION OF THE ISOLATION EFFICIENCY OF VIBRATION COUNTERMEASURES FOR A DOUBLE-DECK TUNNEL

Arnau Clot[1], Robert Arcos[1], Jordi Romeu[1], Behshad Noori[2]

[1] Departament d'Enginyeria Mecànica, Universitat Politècnica de Catalunya, Terrassa, España
{arnau.clot@upc.edu, robert.arcos@upc.edu, jordi.romeu@upc.edu}
[2] AV Ingenieros
{behshad.noori@avingenieros.com}

Abstract
Double-deck tunnels are an innovative tunnel design that has been recently implemented in some underground railways and metro lines worldwide. However, due to the complexity of this type of structures, its dynamic response has not yet been fully comprehended. This lack of understanding complicates the design of efficient vibration isolation countermeasures for them. Therefore, proper models for predicting the vibration impact of double-deck tunnels are highly needed. The aim of this paper is to present, on the one hand, an efficient model of a railway superstructure implemented in a double-deck tunnel and, on the other, to study how the vibration impact of this structure is affected by the addition of an elastomeric mat between the interior floor-tunnel contact and by modifications of the rail pads stiffness and damping values. In both cases, the results are presented in terms of the energy flow radiated upwards by the structure when harmonic moving loads circulate along the rails.

Keywords: vibration impact, double-deck tunnel, energy-flow, rail pad, elastomeric mat.

PACS no. 46.40.-f, 62.30.+d

1 Introduction

The construction of underground railways and metro lines has been constantly growing in the last decades. The high economical cost of their construction and modification has led to the development of new tunnel designs in order to optimize them. One of these innovative designs, implemented in Line 9 of the Barcelona underground railway system, is the double-deck tunnel, in which the tunnel structure is divided into two parts by an intermediate floor supported on the tunnel walls. However, the vibration impact of this structure cannot be properly represented by most of the existing predictive models, which are usually focused to predict the response for simple tunnels.

One of the most important semi-analytical models for predicting the ground-borne vibrations caused by underground railways is the Pipe-in-Pipe (PiP) model presented by Forrest and Hunt [1], [2]. Over the last years the model has been significantly extended and used to perform a wide variety of studies, being particularly interesting the works of Hussein and Hunt, who added a new floating slab model to the system [3] and who also proposed a method, based on the computation of the radiated power flow, for evaluating the variations of the response of underground railways under design modifications [4]. An alternative type of evaluation has been presented by Lopes et al. [5], [6], who developed a numerical model of the tunnel/soil/building system and used it for studying the effect that modifying

the soil stratification and changing the under slab mat stiffness has on the response. The first semi-analytical double-deck model presented in the literature coupled the PiP model to a infinite strip plate model [7]. The model was used by Clot et al. [8] to compare the power flow radiated by a double-deck tunnel structure with that radiated by a simple tunnel in plane strain conditions.

In this work, a superstructure model composed of rails directly fixed to the tunnel interior floor is added to the double-deck tunnel model [7]. The remainder of the paper is structure as follows: The proposed model and energy flow computation are briefly described in section 2. The results for the elastomeric mat and rail pad modifications are presented in section 3. Finally, the conclusions of the work are detailed in section 4.

2   Model description

The model used for describing the dynamic response of a double-deck tunnel structure embedded in a homogeneous soil is schematised in Figure 1. The model considers the following assumptions:

- **Superstructure**: The rails are represented as Bernoulli-Euler beams of infinite length. Both rails are coupled to the tunnel's interior floor with direct fixation fasteners. The rail pads are modelled as a continuous layer with a constant stiffness per metre k_F and a constant viscous damping per metre c_F. Two vertical harmonic point loads moving at a constant speed v_t are assumed to be applied at both rails.

- **Interior floor**: The interior floor is considered as an infinite thin strip plate of constant cross-section. The rails are centred in the interior floor and separated a distance d_r. The coupling between the interior floor and the tunnel structure is performed using the receptance method. An elastomeric mat is implemented between the interior floor and the tunnel structure at the tunnel-floor joining positions. The mat is modelled as a continuous layer with a constant stiffness per metre k_M and a constant viscous damping per metre c_M.

- **Tunnel and soil**: The soil and the tunnel are modelled using the PiP model [1]. The initial formulation of this well-established model considers the tunnel structure as an infinite thin cylindrical shell and the soil as a homogeneous viscoelastic full space.

With the considered formulation, the response of the system to a harmonic moving load of the form

$$p(x,t) = p_0 \cos(\widetilde{\omega}t)\,\delta(x - v_t t) \tag{1}$$

can be expressed as

$$u(0,t) = \frac{1}{(2\pi)^2 v_t} \mathrm{Re}\left[\int_{-\infty}^{\infty} H\left(\frac{\omega - \widetilde{\omega}}{v_t}, \omega\right) \mathrm{e}^{i\omega t}\mathrm{d}\omega\right], \tag{2}$$

where $\widetilde{\omega}$ is the excitation angular frequency, v_t is the load speed and where H is the response of the double-deck tunnel model to two vertical harmonic loads of amplitude 0.5 N applied on both rails expressed in the wavenumber-frequency domain [7]. The cross-section $x = 0$ m has been chosen for simplicity.
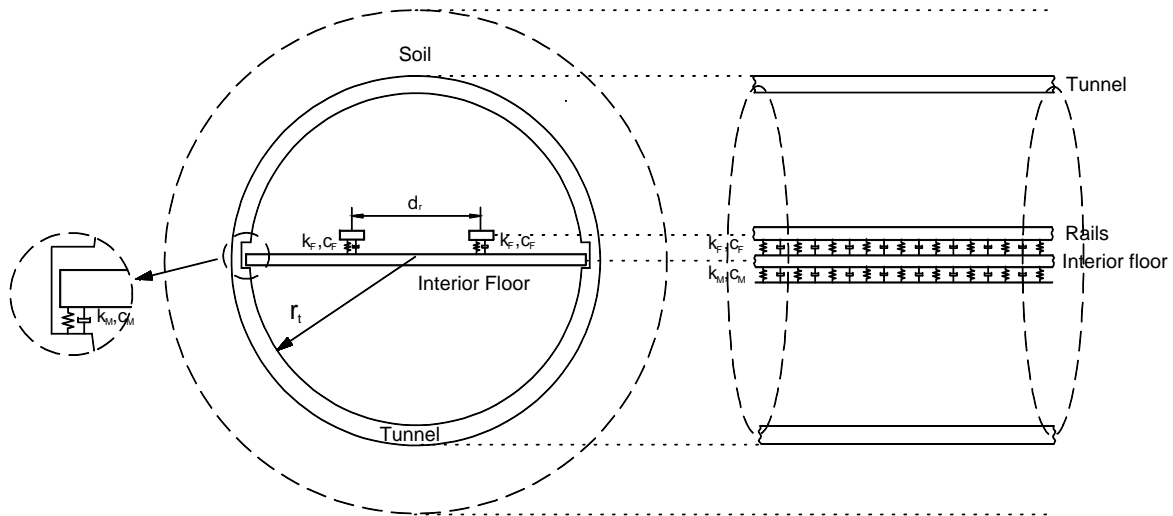
Figure 1 - The proposed double-deck tunnel model.

Rather than using the response of a particular point of the soil, the isolation efficiency of the considered vibration countermeasures is studied by computing the total energy radiated upwards due to the harmonic moving point load excitation. This result is obtained computing the power flow radiated across the surface represented in Figure 2 during the load circulation. The radiated energy can be expressed as

$$E = \int_{-\infty}^{\infty} P(t)\mathrm{d}t, \tag{3}$$

where $P(t)$ is the total power flow radiated upwards, which is obtained from

$$P(t) = r_m \Delta x \int_0^{\pi} \boldsymbol{v}(\theta,t) \cdot \boldsymbol{\tau}(\theta,t)\mathrm{d}\theta, \tag{4}$$

where r_m is the measuring radius, Δx is the width of the considered cylindrical strip surface and where $\boldsymbol{v}(\theta,t)$ and $\boldsymbol{\tau}(\theta,t)$ are the velocity and stress fields of the soil, which are obtained from similar expressions to that defined for the displacement field [7].
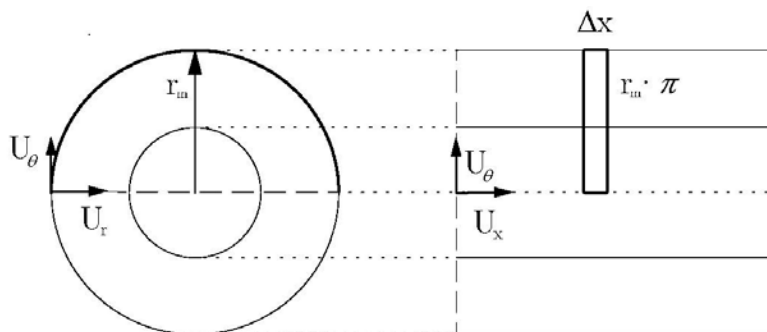

Figure 2 – Chosen surface for computing the radiated energy flow.

3   Results

3.1   Initial considerations

The response to the dynamic excitation caused by a train pass in a fixed position of the soil is obtained as the summation of the response at this point to each axle load $g_{axle}(\widetilde{\omega})$ [9]. Each one of these contributions is computed as the product of $g_{axle}(\widetilde{\omega})$ by the response of the soil to a unitary harmonic moving point load $H\left(\frac{\omega-\widetilde{\omega}}{v_t}, \omega\right)$. Therefore, the variation of the soil response due to a modification of any of the system parameters would be caused by the combination of the variations caused in both terms. The studies performed in this work are focused on determining the effect caused in $H\left(\frac{\omega-\widetilde{\omega}}{v_t}, \omega\right)$ by a modification of the elastomeric mat and rail pads stiffness and damping values. Due to the fact that the dynamic axle loads are also affected by these modifications, the obtained results cannot be directly understood as reductions or amplifications of the soil vibrations caused by a train pass. Although it is expected that the dynamic axle loads would not be significantly affected by a change in the elastomeric mat parameters, they may change considerably if the rail pad stiffness is modified.

The geometrical and mechanical parameters considered in all the calculations are presented in Table 1 and Table 2. Details regarding the model computation can be found in [7].

Table 1 – Rail and interior floor parameters.

Rail Parameters	Value	Floor Parameters	Value
Cross-sectional area	$6.93 \cdot 10^{-3}$ m^2	Width	10.9 m
Second moment of area	$23.5 \cdot 10^{-6}$ m^4	Thickness	0.4 m
Young modulus	207 GPa	Young modulus	25 GPa
Density	7850 kg/m^3	Poisson ratio	0.175
Rails distance	1.8 m	Density	3000 kg/m^3

Table 2 – Tunnel and soil parameters.

Tunnel Parameters	Value	Soil Parameters	Value
Radius	5.65 m	Density	2000 kg/m^3
Thickness	0.4 m	Poission ratio	0.3
Young modulus	27.6 GPa	Young modulus	150 MPa
Poisson ratio	0.175	P-wave damping	0.03
Density	3000 kg/m^3	S-wave damping	0.03

3.2   Elastomeric mat between the floor and the tunnel

This section evaluates the effect that a modification of the elastomeric mat stiffness and damping values has on the energy radiated by the double-deck tunnel structure.

Figure 3 shows the frequency spectrum of the soil's radial velocity field V_r and soil's radial stress field T_{rr} at $r_m = 10$ m and $\theta_m = \pi/2$ for two different load speeds, $v_t = 16$ m/s (subplots (a)-(b)) and 32 m/s (subplots (c)-(d)), and for an excitation frequency $f_e = \frac{\widetilde{\omega}}{2\pi} = 60$ Hz. In each case, the results for three different values of the elastomeric mat stiffness ($k_M = 2.5$, 10 and 40 MN/m^2) have been compared. In all cases a viscous damping $c_M = 12$ kN·s/m^2 has been considered. The results state the importance of the Doppler effect, which spreads the spectrum of the soil response along a range of frequencies

around the excitation one. It can be observed that the width of this frequency range increases with the load speed and that the response is not symmetric respect to the excitation frequency. This range is in agreement with the frequency range of interest defined, for example, in [9]. The results show that both frequency spectra are clearly affected by a modification of the elastomeric mat stiffness value.
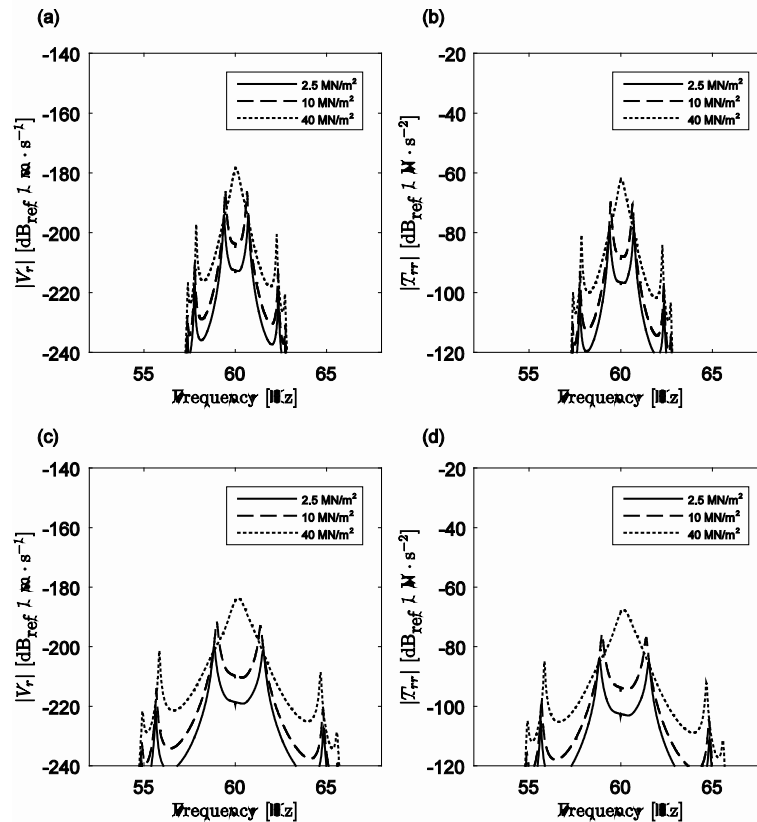

Figure 3 – Soil radial velocity field and radial stress field spectra for f_e= 60 Hz and for v_t= 16 m/s (subplots (a)-(b)) and 32 m/s (subplots (c)-(d)). Three different elastomeric mat stiffness values have been considered.

Figure 4 shows the power flow radiated upwards for two different load speeds (16 m/s in the upper subplots and 32 m/s in the lower ones) and two different excitation frequencies (20 Hz in the left subplots and 60 Hz in the right ones). The results have been computed using Eq. (4) for r_m= 10 m and $\Delta x = 1$ m. Only the case k_M= 2.5 MN/m^2 has been considered. The results show that the amplitude of the power flow clearly depends on the considered excitation frequencies but it is almost not affected by an increase in the load speed.

Figure 5 presents the energy radiated upwards for excitation frequencies in the frequency range of interest (1-80 Hz). The results are presented for the three elastomeric mat parameters previously used and for two different load speeds: 16 m/s (a) and 32 m/s (b). The results show that the total energy radiated is significantly affected by the stiffness of the floor-tunnel contact. For excitation frequencies over 20 Hz, the softest elastomeric mat is clearly the best option for reducing the energy radiated upwards by a moving harmonic load. Less clear is the response of the system between 5 and 20 Hz, where the responses of the three considered mats are highly variable. Similar results have been obtained for both load speeds.
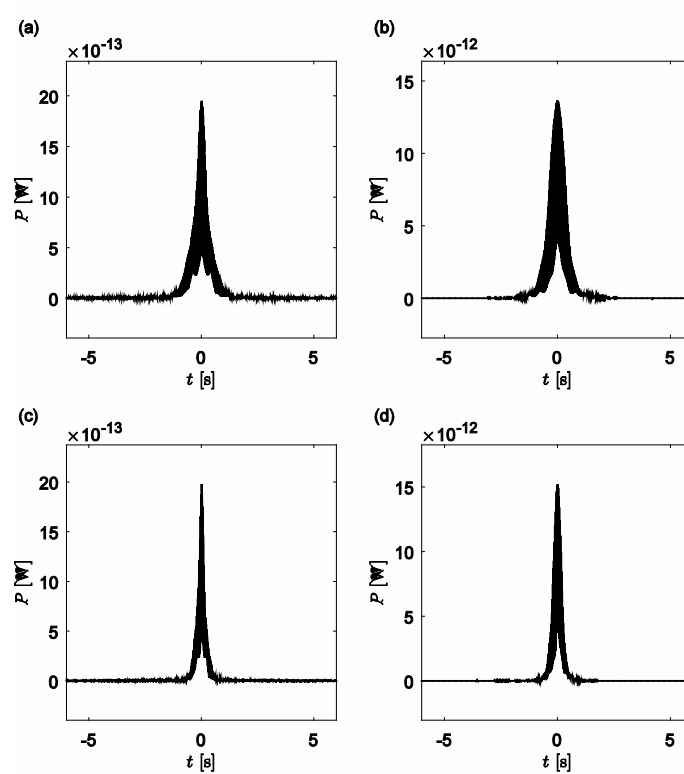
Figure 4 – Power flow radiated upwards for: (a) f_e= 20 Hz and v_t= 16 m/s, (b) f_e= 60 Hz and v_t= 16 m/s, (c) f_e= 20 Hz and v_t= 32 m/s and (d) f_e= 60 Hz and v_t= 32 m/s.

In order to quantify the isolation efficiency that can be obtained by modifying the elastomeric mat mechanical parameters, the previous energy flow radiated upwards is integrated from 1 to 80 Hz. The resulting total energy E_T can be understood as the energy radiated by an excitation which is equal to a white noise of unitary amplitude from 1 to 80 Hz. An insertion loss factor IL is defined as

$$IL = 10 \log_{10} \left(\frac{E_{T,\max}}{E_T} \right), \qquad (5)$$

where $E_{T,\max}$ is the maximum value of the total energy radiated upward for the range of elastomeric mat parameters considered.

Figure 6(a) shows the IL computed for k_M values between 2 and 200 MN/m^2 and c_M values between 1 and 100 kN·s/m^2. The results obtained for the particular case where c_M has been fixed to 1.9 kN·s/m^2 (dotted line) and c_M = 13.9 kN·s/m^2 (dashed line) have been also presented in subfigures (b) and (c), respectively. As can be observed in the results, the isolation efficiency of the elastomeric mat has a complex dependence on the considered properties, being, in general, higher for smaller values of c_M. For the studied case, the maximum IL is obtained for k_M= 14.4 MN/m^2 and c_M= 72 kN·s/m^2. It is important to mention that the current study is not considering how feasible is to obtain an elastomeric material with these mechanical characteristics.
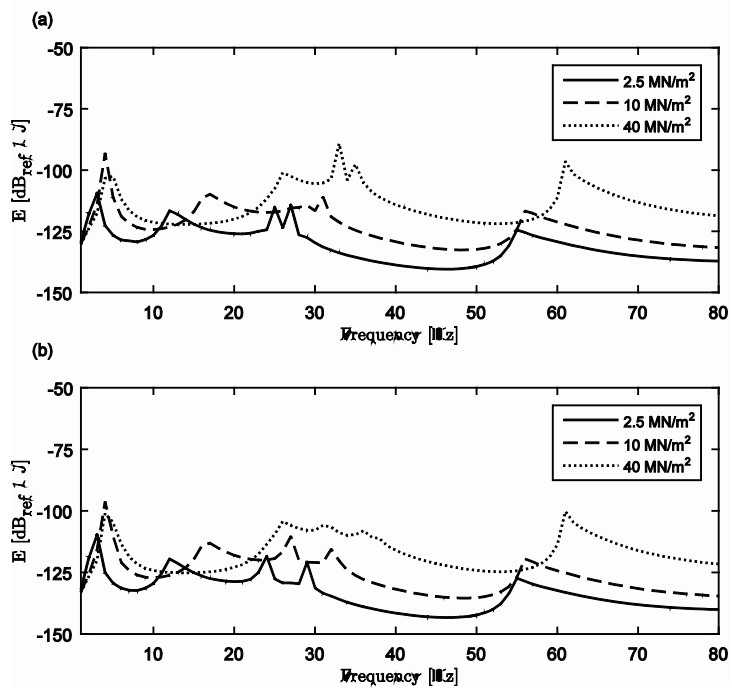
Figure 5 - Energy flow radiated for three different values of the elastomeric mat stiffness. (a) v_t= 16 m/s. (b) v_t= 32 m/s.
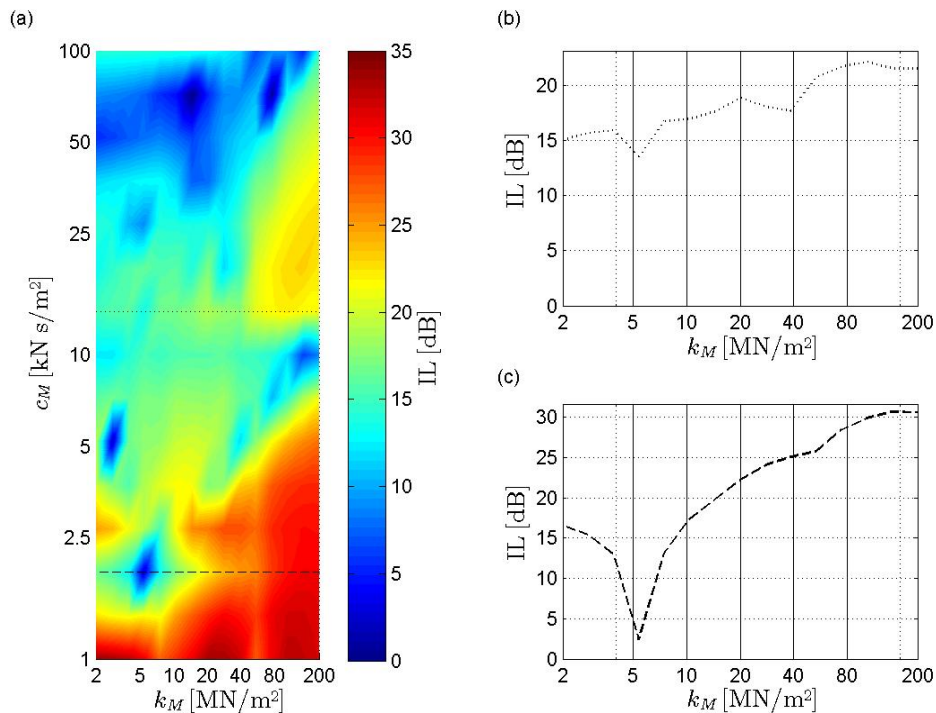

Figure 6 –IL obtained modifying the elastomeric mat parameters. (a) Results for a wide range of stiffness and damping values. (b) Results for c_M= 13.9 kN·s/m^2. (c) Results for c_M= 1.9 kN·s/m^2.

3.3 Rail pads stiffness

This section presents the results obtained when the stiffness and damping of the rail pads are modified. Because the results obtained are analogous to the elastomeric mat ones, its computation details are just briefly described and only the results regarding the total energy flow radiated upwards for different values of the rail pads stiffness and viscous damping are presented.

In Figure 7 the energy radiated upwards is computed for three different k_F values: 10, 50 and 250 MN/m^2 and for two different load speeds: 16 m/s (a) and 32 m/s (b). A viscous damping $c_F = 30.0$ kN·s/m^2 has been considered in all cases. The results show that the effect of modifying the rail pads stiffness is only appreciable for excitation frequencies over 20 Hz, being the difference less than 5 dB in the whole range of frequencies studied.
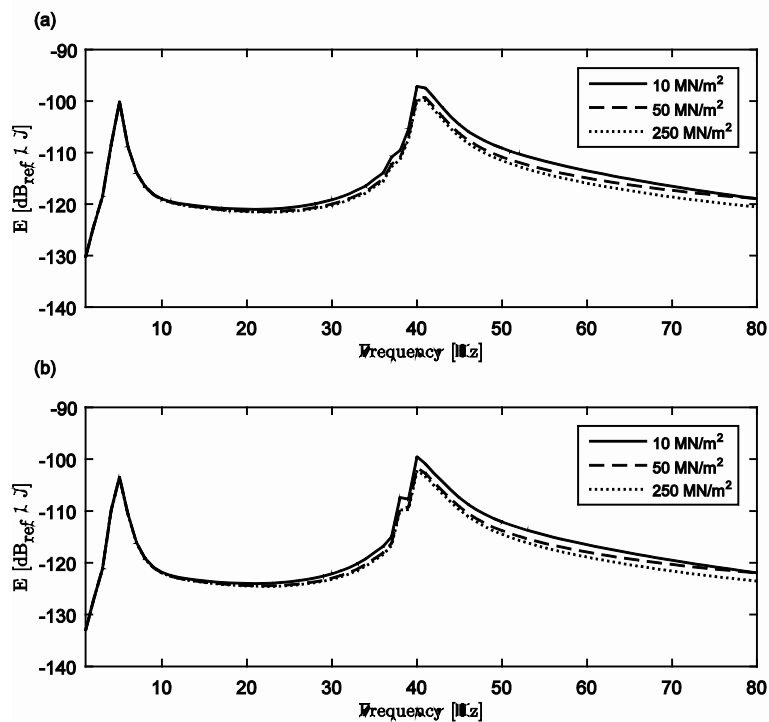

Figure 7 – Energy flow radiated for three different values of the rail pad stiffness. (a) v_t= 16 m/s and (b) v_t= 32 m/s.

The results presented in Figure 8 show the IL obtained for k_F values between 5 and 500 MN/m^2 and c_F values between 1 and 100 kN·s/m^2. The results obtained for the particular case where c_F has been fixed to 1.7 kN·s/m^2 (dotted line) and the case where has been fixed to $c_F = 13.0$ kN·s/m^2 (dashed line) have been also presented in subfigures (b) and (c), respectively. The results show that, while the IL is significantly reduced for small values of the damping and stiffness coefficients, for larger values of the damping coefficient it is almost not affected by a modification of the rail pad stiffness. This result indicates that the rail pad isolation efficiency cannot be properly quantified without taking into account its effect in the magnitude of the wheel-rail contact forces. In order to do this, a vehicle dynamic model has to be coupled to the track/tunnel/soil model presented. The next step of the authors' study is to perform this coupling.
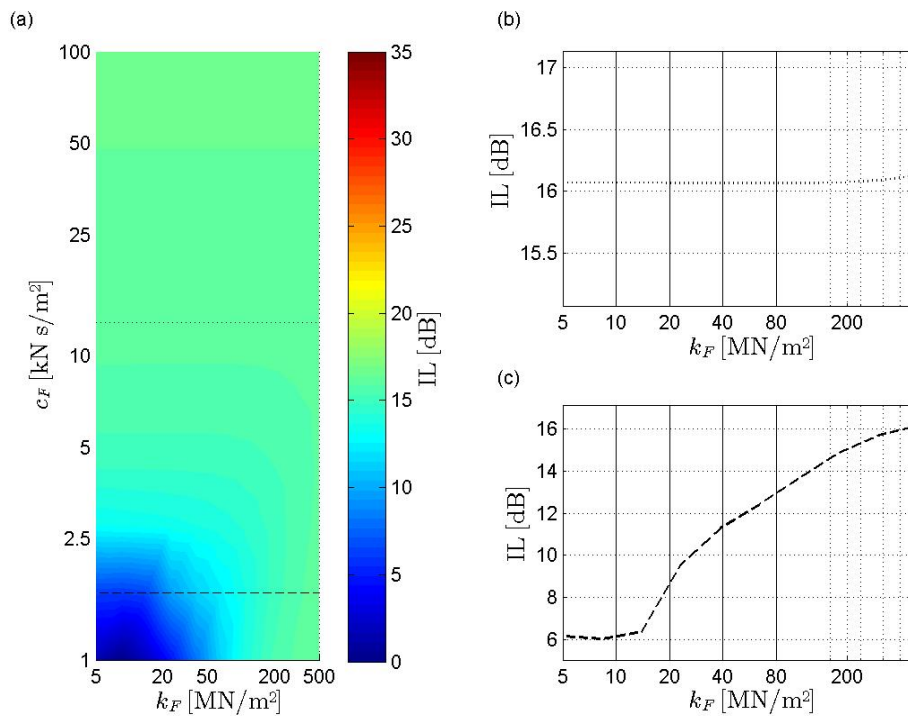
Figure 8 – IL obtained modifying the rail pads parameters. (a) Results for a wide range of stiffness and damping values. (b) Results for c_F= 13.0 kN·s/m². (c) Results for c_F= 1.7 kN·s/m².

4   Conclusions

This work presents an evaluation of the isolation efficiency of two vibration countermeasures potentially applicable in a double-deck tunnel structure: The addition of an elastomeric mat at the interior floor-tunnel joining positions and the modification of the rail pads mechanical parameters. These evaluations have been performed computing the energy flow radiated by the structure when it is excited by harmonic moving loads. A semi-analytical model of the coupled system rails/double-deck tunnel/soil has been used for performing these calculations.

It has been found that, for the tunnel and soil parameters considered, the modification of the elastomeric mat properties resulted into significant variations of the radiated energy. In particular, the results have shown that the maximum attenuation is obtained for small damping values and rather small stiffness values. The variations observed in the response also highlight the importance of having the mechanical parameters of the system well characterised.

On the other hand, small variations of the radiated energy have been found when the rail pad parameters have been modified. A reduction of its isolation efficiency has been obtained for very small values of its stiffness and damping values. This result indicates that an adequate quantification of the rail pads isolation efficiency requires taking into account how the wheel-rail interaction forces

are affected by a change in the rail pads parameters. The authors are currently working in the development of a coupled vehicle/track model that will be used for studying this effect.

Acknowledgements

References

[1]   Forrest, J. A.; Hunt, H. E. M. A three-dimensional tunnel model for calculation of train-induced ground vibration. *J. Sound Vib.*, Vol 294(4), pp 678–705.

[2]   Forrest J. A.; Hunt, H. E. M. Ground vibration generated by trains in underground tunnels. *J. Sound Vib.*, Vol. 294(4–5), pp 706–736.

[3]   Hussein, M. F. M.; Hunt, H. E. M. A numerical model for calculating vibration from a railway tunnel embedded in a full-space, *J. Sound Vib.*, Vol. 305(3), pp 401–431.

[4]   Hussein, M. F. M.; Hunt, H. E. M. A power flow method for evaluating vibration from underground railways, *J. Sound Vib.*, Vol 293(3–5), pp. 667–679.

[5]   Lopes, P.; Alves Costa, P.; Calçada, R.; Silva Cardoso, A. Influence of soil stiffness on building vibrations due to railway traffic in tunnels: Numerical study, *Comput. Geotech.*, Vol 61, pp 277–291.

[6]   Lopes, P.; Alves Costa, P.; Ferraz, M.; Calçada, R.; Cardoso, A. S. Numerical modeling of vibrations induced by railway traffic in tunnels: From the source to the nearby buildings, *Soil Dyn. Earthq. Eng.*, Vol 61–62, pp. 269–285.

[7]   Clot, A. *A dynamical model of a double-deck circular tunnel embedded in a full-space*. PhD thesis. Universitat Politècnica de Catalunya.

[8]   Clot, A.; Romeu, J.; Arcos, R.; Martín, S. R. A power flow analysis of a double-deck circular tunnel embedded in a full-space, *Soil Dyn. Earthq. Eng.*, Vol. 57, pp. 1–9.

[9]   Lombaert, G.; Degrande, G.; Ground-borne vibration due to static and dynamic axle loads of InterCity and high-speed trains, *J. Sound Vib.*, Vol. 319(3–5), pp. 1036–1066.